

# Effect of Microstructure and Chemical Composition of Hardfacing Alloy on Abrasive Wear Behavior

Sanjay Kumar, D.P. Mondal, and A.K. Jha

(Submitted 11 April 2000; in revised form 28 June 2000)

**Hardfacing, a surface modification technique, is used to rebuild the surface of a workpiece. The economic success of the process depends on selective application of hardfacing material and its chemical composition for a particular application. In this context, three hardfacing electrodes having different chemical compositions have been selected and their abrasive wear responses was compared with that of mild steel. The emphasis has been made to realize the effect of microstructure and chemical composition on the wear response of the hardfacing material with respect to mild steel. It has been observed that the wear rate of hardfacing alloys is lower than that of mild steel. The hardfacing alloy having the highest chromium content exhibits the lowest wear rate.**

**Keywords** hardfacing materials, HVOF spraying, surface engineering, tribology, wear

## 1. Introduction

Among the surface modification techniques used in engineering applications, hardfacing probably is the most common one to improve the wear resistance of the components.<sup>[1–8]</sup> Hardfacing primarily involves deposition of a hard, wear-resistant material to the specific areas of the surface of the components by any of the techniques such as welding, thermal spraying, high velocity oxy-fuel (HVOF) spraying, plasma spraying, *etc.* A number of hardfacing materials are available, and the proper choice has to be made depending on the alloy chemistry, area of application, and the cost factor.<sup>[8,9]</sup> Agricultural and mining implements are subjected to extensive wear due to abrasion, erosion, and impact, and, hence, hardfacing may be employed on the surface of these implements for improving the life of such components. Hardfacing can even be employed in used components to restore the life of such components. In the present investigation, hardfacing materials of three different compositions have been selected for overlaying of the soil-engaging part of agricultural implements that are generally made of mild steel. As these components are subjected to abrasive wear against the soil, the present investigation also aims to assess the high-stress abrasive wear of three hardfacing alloys as compared to that of the mild steel. To understand the wear mechanism, the wear surfaces were examined under a scanning electron microscope (SEM).

## 2. Experimental Procedure

### 2.1 Material Composition and Hardness

Overlaying material of three different chemical compositions and mild steel were used in this present study. The composition

of mild steel and overlaying materials is reported in Table 1. This table also includes the hardness of these materials. The materials have been given their respective code names as reported in Table 1. In the following sections, these code names will be used for discussion.

### 2.2 Hardfacing Technique

In the present investigation, hardfacing was performed by the open arc welding technique. In this process, an arc is established between the hardfacing electrode and workpiece (substrate). The workpiece is made of mild steel. The arc is moved along the substrate with subsequent melting and fusing of the metal (workpiece and electrode). The molten electrode is deposited over the fused substrate. Since the arc is the hottest source of heat and the molten electrode is deposited over the fused (partially melted) metal substrate, this results in fusion as well as diffusion bonding between workpieces and hardfacing material. A weld deposit up to 1 to 2 mm thickness has been made on the substrate for each composition of overlaying materials. This thickness is achieved by depositing electrode materials in number of passes where the desired thickness is not achieved in single pass.

### 2.3 Specimen Preparation

Specimens have been prepared for a high-stress abrasion test as well as for microstructural observations. Specimens for the high-stress abrasive wear test of all these types of overlaying material and mild steel are  $40 \times 35 \times 4$  mm. The specimens of specific size have been cut and subsequently ground and polished to obtain a smooth surface from either side for good contact with abrasive media during wear testing. The specimens having the size of  $4 \times 6 \times 6$  mm of overlaying material and mild steel substrate for their microstructural observation have been prepared by cutting the material from the weld pool. The specimens were metallographically polished and etched (with 3% nital solution) before examination under an optical microscope. The worn surfaces of the specimen were also prepared by cutting the specimen of the size of  $6 \times 6 \times 4$  mm from

Sanjay Kumar, D.P. Mondal, and A.K. Jha, Regional Research Laboratory (CSIR), Bhopal-462 026, India. Contact e-mail: root@rlbpl.mp.nic.in.

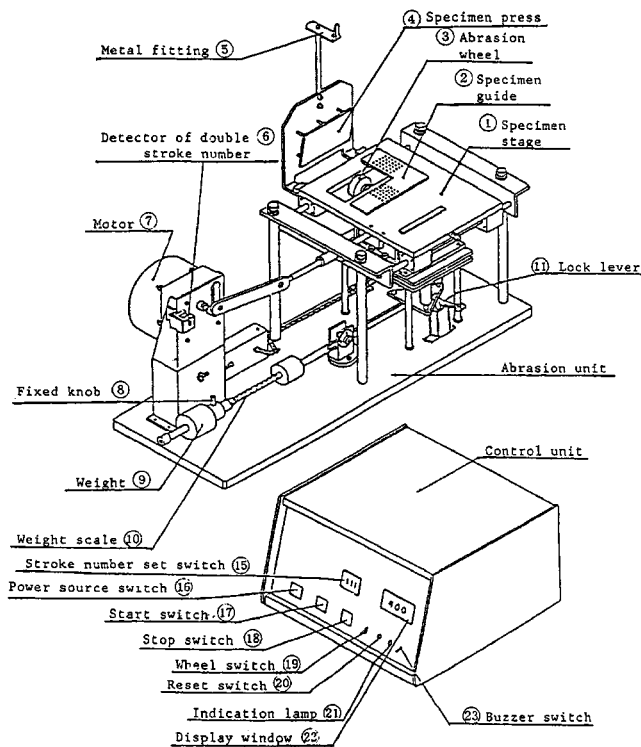


Fig. 1 Schematic diagram of suga abrasion tester

Table 1 Chemical composition and hardness of mild steel and hardfacing materials

Solution number	Material	Hardness (Hv)	Compositions (wt.%)					
			C	Mn	Si	Cr	Mo	Fe
1	Mild steel	162	0.32	...	0.40	...	...	Rem
2	Composition 1	705	0.50	0.3	0.45	6.5	...	Rem
3	Composition 2	252	0.20	1.0	0.35	1.0	0.5	Rem
4	Composition 3	250	0.20	0.4	0.40	1.8	...	Rem

the worn region after abrasion tests. The specimens were sputtered with gold prior to SEM examinations.

### 2.4 Two-Body Abrasive Wear Test

This test has been conducted on the metallographically prepared sample using a Suga Abrasion Tester (model NUS-1, Tokyo, Japan). The schematic view of the apparatus is shown in Fig. 1. In this test, specimens were fixed on the platform. The platform along with the specimen was subjected to reciprocating motion against a rotating wheel on which abrasives (SiC grit paper) were fixed. The samples were subjected to load by a cantilever mechanism. The wheel, on which abrasive paper was fixed, rotates slowly. One rotation of the wheel is completed while 400 strokes (each stroke corresponding to 1 cycle of reciprocating motion that covers a distance of 0.045 m) of the specimen are completed. Each 400 strokes corresponds to 26 m of distance traveled by the specimen. The wear rates of the specimen have been calculated by weight-loss measurement

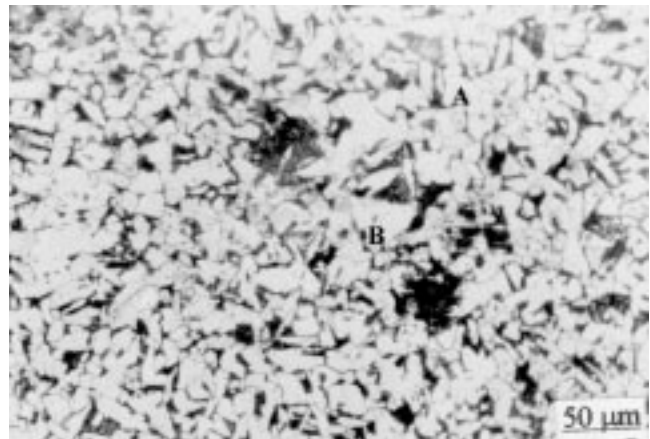


Fig. 2 Microstructure of mild steel

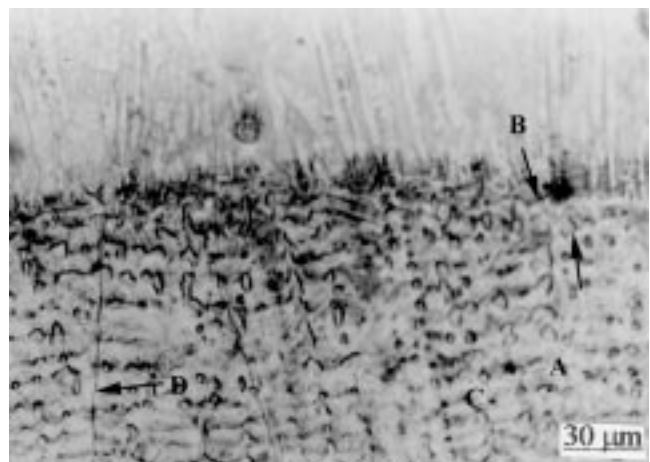


Fig. 3 Microstructure of hardfacing material of composition 1

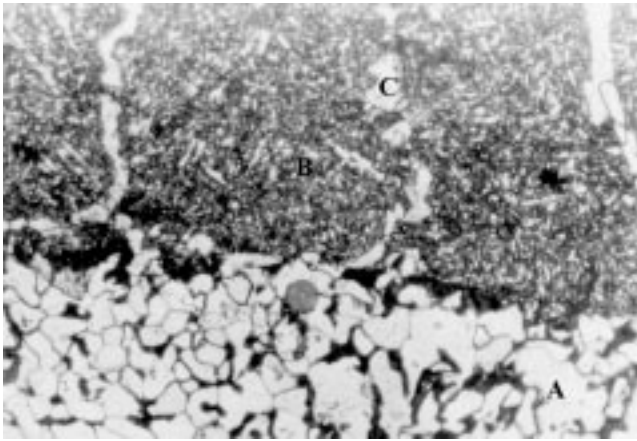
technique. The abrasion tests have been conducted at a load of 7 N over a sliding distance of 182 m against a SiC abrasive media having an abrasive size of 52  $\mu\text{m}$ . The tests were conducted using the same abrasive for the entire sliding distance.

## 3. Results and Discussion

### 3.1 Material and Microstructure

The microstructure of mild steel as shown in Fig. 2 indicates the presence of a pearlitic phase (marked "A") in the matrix of ferrite (marked "B"). The grains are found to be elongated longitudinally, which indicates that the steel is received in hot-worked condition. It is noted from the microstructure that the mild steel contains about 35% pearlitic phase and the rest ferrite. This is well in agreement with the theoretically calculated value of pearlitic volume fraction from the Lever rule using the Fe-C diagram. Due to the larger fraction of the ferrite phase, which is a relatively softer phase, mild steel has lower hardness, *i.e.*, 162 Hv,<sup>[4,7-9]</sup> as compared to the overlaying materials (Table 1).

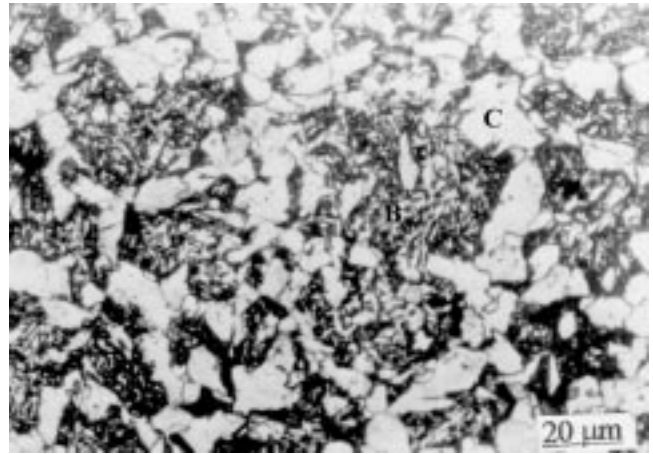
The microstructure of interfaces (marked "arrow") between first (marked "A") and second passes (marked "B") of overlaying of composition 1 is shown in Fig. 3. It is evident from this



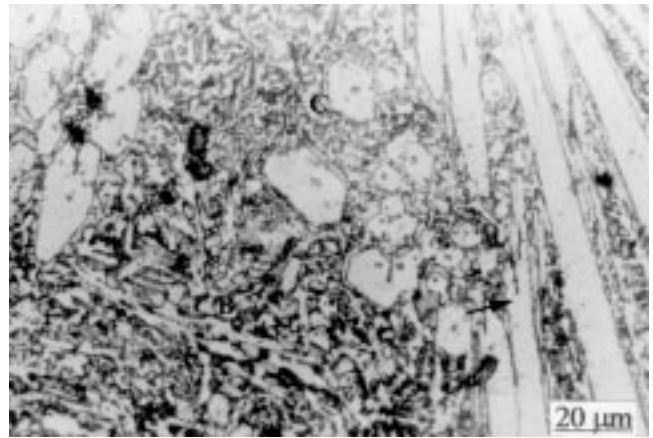
**Fig. 4** Microstructure showing the interface between hardfacing material composition 2 and substrate steel

figure that the bonding between the first and second overlaying is of a diffusion type. Diffusion takes place around the interfaces at very high temperature and particularly at the liquid stage, and thus, the bonding formed between these layers in this process is relatively strong. The absence of any broad bond line is the main feature of this type of bonding, as observed in Fig. 3. The microstructure of the overlaying material of composition 1 shows the dendrites of ferrite (marked “C”) along with primary and secondary carbides (marked “D”) in the interdendritic region and around the dendrites. This is primarily due to a considerably higher amount of chromium (6.5%) and carbon (0.5%) in this overlaying material and solidification of melted overlaid alloy at the steel substrate.<sup>[9]</sup> Because of the chilling effect of the steel substrate, the dendritic structures are noted to be very fine. The presence of higher chromium and higher carbon content results in a relatively larger fraction of fine primary and secondary carbides in the microstructure.

The microstructure of hardfacing material of composition 2 on the mild steel substrate at different locations with respect to interface (between overlaying and substrate) is shown in Fig. 4. It is noted that the bonding (marked “arrow”) between substrate (marked “A”) and overlaying material is reasonably good and of diffusion type, as observed in the case of composition 1. It is also evident from Fig. 4 that, near the bonding line (arrow marked) between mild steel substrate and the overlaying deposit, a bainitic (marked “B”) type of microstructure surrounded by a network of ferrite (marked “C”) is noted in the overlaying of composition 2. The high-magnification microstructure of overlaying material of composition 2 is shown in Fig. 5. It clearly depicts the network of ferrite (marked “C”) around the bainitic colonies (marked “B”). The volume fraction of ferrite is noted to be of the order of 15%. The molten material does not transform to martensite, perhaps because of lower hardenability. As the carbon content is relatively low (Table 1) and ferrite stabilizers such as Cr and Mo are present in small amounts, the ferrite network around the bainitic colonies is noted in this overlaying material. The overlaying material of composition 2 contains a lower amount of the chromium and comparatively higher manganese with 0.5% of Mo. The Mn, Cr, Mo, and Si improve the hardenability of steel, but the hardenability does not reach the extent that steel will give a



**Fig. 5** Microstructure of hardfacing material of composition 2 showing bainitic colonies with ferrite network



**Fig. 6** Microstructure of hardfacing material of composition 3 showing bainitic colonies with ferrite network and Widmanstätten type of structure

martensitic structure in a moderate cooling rate (air cooling); rather, it results in bainitic structure with a network of ferrite. For the same reason, the microstructure of overlaid material for composition 3 (Fig. 6) shows bainitic structure (marked “B”) with ferrite network (marked “C”). In some regions, ferrite moves into bainitic colonies resulting in a Widmanstätten type of microstructure (marked “arrow”) in Fig. 6.

### **3.2 Effect of Microstructure and Chemical Composition on the Wear Behavior of Material**

The wear rates as a function of a sliding distance for different materials at 7 N load are shown in Fig. 7. The wear rates of the overlay materials are lower than that of mild steel. Among the overlaying material, composition 1 exhibits a minimum wear rate. It is also noted that the initial wear rates of all the materials are greater than the wear rate at later stages as the sliding distances progress. The wear rate at the latter stage is considered to be the stable wear rate. This initial wear rate may be considered to be similar to the run-in wear. At the beginning

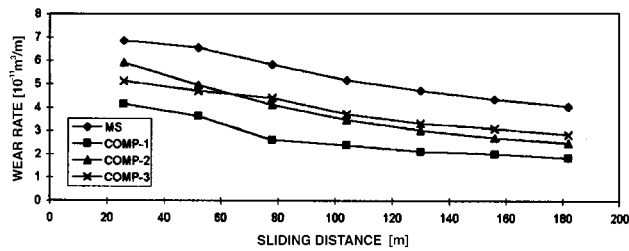


Fig. 7 Wear rate as a function of sliding distance at 7 N load

of the wear process, the contact area between the abrasive particle and the asperities on the specimen surface is relatively low, *i.e.*, a lower number of abrasives are in contact with the specimen surface. This may be because of the fact that the surface may contain sharp asperities to protect the base surface. Thus, the entire load is shared by a few abrasives and this high load is transferred to the few numbers of sharp asperities on the specimen surface. Due to this fact, the effective stress produced by the individual abrasive particle on the sharp asperities of the specimen surface is greater, which leads to significantly high plastic deformation of the asperities vis-à-vis the surface, and the asperities are subjected to fracture; thus, it is expected that more material is removed in this stage, *i.e.*, run-in wear. Additionally, because of higher effective stress on each individual abrasive, they penetrate deeper into the surface and cause more material removal from the individual wear groove. But, at the same time, fewer wear grooves are formed because fewer abrasive particles are taking part in material removal. As a result, the effect of high effective stress on abrasive wear may be balanced by fewer wear grooves, due to fewer abrasives, and, thus, in this case, wear may be invariant to the sliding distance. But in this investigation, tests were conducted using the same abrasive for the entire range of sliding distance. The abrasive particles, thus, generally get blunted, which results in reduction of their cutting efficiency. Additionally, there are chances of detachment of the abrasive particle from the abrasive media (shelling). Some of the material during the wear test is also transferred into the abrasive media either at the tip of the abrasives (capping) or at the interparticle region of the abrasive media (logging). All these factors are also responsible for the reduction in cutting efficiency of the abrasives and, in due course, result in a reduced wear rate.<sup>[10–15]</sup> Some energy is also spent on the plastic deformation of the surface, which causes work hardening of the subsurface, and it may also lead to reduction in wear rate.<sup>[13,14,15]</sup> However, after a specific sliding distance, the effect of all the above factors (shelling, capping, clogging, work hardening, *etc.*) becomes stabilized and produces a stable wear rate at the later stage.

The present study was conducted at fixed load (7 N) and at fixed abrasive size (52 μm). Hence, it is expected that the variation in wear rate in different hardfacing materials is primarily due to the variation in their chemistry, microstructure, and hardness. The wear mechanism may also be different in different hardfacing materials because of these above facts. In the case of softer ones, a ploughing type of mechanism (where larger flakes are generated and some flakes keep on holding along the wear track) is prevailing, but in harder ones, a cutting type of wear mechanism is dominating (where finer cutting chips

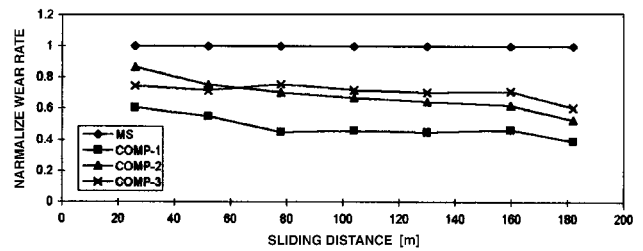


Fig. 8 Normalized wear rate of materials as a function of sliding distance

are generated). The wear rate of overlaying materials of composition 2 and composition 3 are nearly the same. At the initial stage, the wear rate of overlaying material of composition 3 is lower than that of composition 2. But after a specific sliding distance (*i.e.*, 60 m), the wear rate of composition 3 became marginally higher than that of composition 2. In fact, both the overlaying materials, composition 2 and composition 3, have a network of ferrite of the order of 15 to 20% around bainitic colonies and have almost the same chemistry. The overlaying material of composition 2 contains 1% of Cr and 0.5% of Mo, whereas composition 3 contains 1.8% of Cr. The lower amount of Cr in composition 2 is nullified by the presence of the 0.5% of Mo. The Cr and Mo both are ferrite stabilizers. If we consider that 1% of Mo is equivalent to 4% of Cr, the overall effect of the alloying element in composition 2 becomes higher than that of composition 3. Furthermore, Mo-carbides are significantly harder and more thermally stable than Cr-carbides. As a result, composition 2 gives relatively finer and harder bainites and it exhibits higher hardness than composition 3. Additionally, the Widmanstätten type of structure makes composition 3 very brittle, which may facilitate a higher wear rate in composition 3. The overlaying materials of composition 1 contain a significantly higher amount of Cr (6.5%), which possibly causes formation of larger amounts of primary and secondary carbides ( $M_3C_7$ ,  $M_7C_3$ ) in the ferrite matrix, where M stands for metals such as Cr, Mo, *etc.* These hard carbides and finer dendritic structures lead to significantly higher hardness vis-à-vis lower wear rate in composition 1 as compared to other compositions. The significantly lower wear rates of compositions 2 and 3 as compared to that of mild steel may be due to their ferrito-bainitic structure, which is harder as well as tougher than the ferrite-pearlitic structure.

The wear rate of the materials was normalized with respect to the wear rate of the mild steel. The normalized wear rate (NWR) is defined, here, as follows:

$$NWR = \frac{\text{Wear rate of specific material}}{\text{Wear rate of mild steel}}$$

Thus, the NWR of mild steel becomes unity and remains invariant to the sliding distance. The NWR values of the materials are plotted against sliding distance in Fig. 8 to examine the relative effect of overlaying materials over mild steel. The NWR of other materials is also noted to be more or less invariant to sliding distance, except in the very initial stage or at the latest stage. However, these analyses clearly assess the comparative wear rate of different materials. It is noted that the wear rate

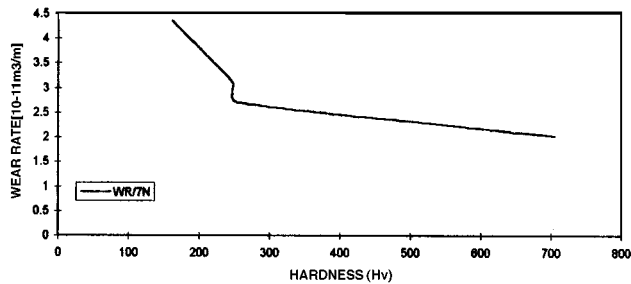


Fig. 9 Wear rate of materials as a function of their hardness

of the overlaid material of composition 1 is almost 0.4 times the wear rate of mild steel. Similarly, the wear rates of compositions 2 and 3 are 0.65 and 0.7 times, respectively, that of mild steel. The above calculation clearly demonstrates that the wear rate of composition 1 is 0.66 times the wear rate of composition 2 or composition 3, even though the hardness of composition 1 is almost three times higher than that of composition 2 or composition 3.

The hardness of a material may be an important factor in controlling the abrasive wear behavior of the material. The stable wear rate of different materials at 7 N load is plotted as a function of their hardness in Fig. 9. It is noted that the wear rate decreases with an increase in hardness value, but does not follow any linear relationship with hardness of the materials. This is in agreement with earlier reports where the cutting type of wear mechanism is dominating.<sup>[13–17]</sup> The abrasive particle under load penetrates into the surface of the material, and, due to reciprocating motion, the penetrated particles cause scratching on the specimen surface by cutting or ploughing. The subsurface deformation may also be taking place, but the extent of deformation is less in abrasive wear because material is removed by the cutting or ploughing action of the abrasives. Due to deformation, very minor cracking on the subsurface is taking place, which is not growing to critical length. Thus, wear due to deformation becomes insignificant as compared to that due to cutting or ploughing.

It may be noted that, initially, the wear rate decreases very rapidly with the increase in hardness. But the rate of reduction of the wear rate decreases when hardness becomes more than 249 Hv. This may be due to the different mechanism of wear acting on the specimen surface depending on their hardness and microstructures. It was mentioned earlier that when the hardness is high (composition 1), generally, fine machining chips are produced and subsequently removed from the specimen surface. But the depth of cut is less and, hence, causes a very low wear rate. When hardness is low enough (*i.e.*, mild steel), the depth of cut is relatively high and results in very long continuous fibrous chips and, thus, results in a significantly higher wear rate. The depth of cut also depends on the effective contact, which is again dependent on surface and subsurface characteristics. The depth of cut by the abrasive is reduced significantly when the hardness of the material reaches the order of 249 Hv. This may also be due to the occurrence of the bainitic phase (which is harder as well as tougher) in compositions 2 and 3. This phase covers a large part of the material and, hence, protects the abrasive from coming in contact effectively with the specimen surface. The depth of cut

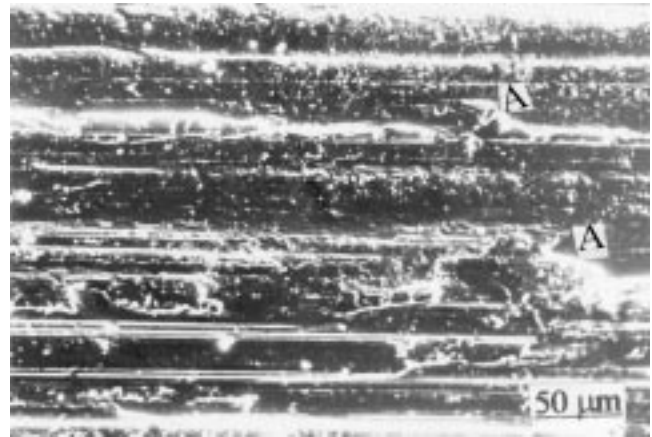


Fig. 10 Micrograph of the wear surface of hardfacing material of composition 1

may be reduced marginally with an increase in hardness above 250 Hv. The harder carbides in composition 1 may be protecting the surface from the destructive action of the abrasive. But the extent of reduction of contact between the abrasive and the specimen surface and the depth of penetration of the abrasive to the specimen do not reach to the level expected from the increase in hardness over other materials. This is primarily due to the significantly finer (maximum 5  $\mu\text{m}$ ) carbides, as compared to the abrasive size, which improves the hardness of the material considerably, not being able to effectively protect the specimen surface from the coarser abrasive. This signifies that microstructural features of the hardfacing material play an important role with the hardness to control their wear behavior.

### 3.4 Microscopy of Wear Surface

Different types of wear mechanisms may exist depending upon the nature of microstructure and hardness of the material. The micrographs of the worn surface of the specimens, *i.e.*, mild steel and all the overlaying materials, are examined to assess the prevailing wear mechanism. The wear surface of mild steel (Fig. 10) shows the deeper and wider grooves, more damaged regions, relatively larger flaky materials (marked arrow) along the wear track, and entrapment of detached abrasives (marked A) that cause deep pits or scratches in subsequent passes. This indicates the ploughing type of wear mechanism is prevailing in mild steel. In contrast, significantly finer, shallower, and more continuous wear grooves and considerably less flaky materials along the wear track of composition 1 (as shown in Fig. 11) indicate that microcutting is the dominating wear mechanism in composition 1. The wear surfaces of compositions 2 and 3 as shown in Fig. 12 and 13, respectively, indicate moderate depth and width of wear grooves with small flakes along the wear track. These suggest that both ploughing and microcutting mechanisms are equally responsible for the wear of materials. Small pits in Fig. 12 and 13 (marked B) may be due to entrapment of abrasives and material removal in subsequent passes.

During abrasive wear, the specimen is subjected to reciprocating motion against the abrasive media. The abrasion causes continuous wear grooves due to cutting and ploughing of the

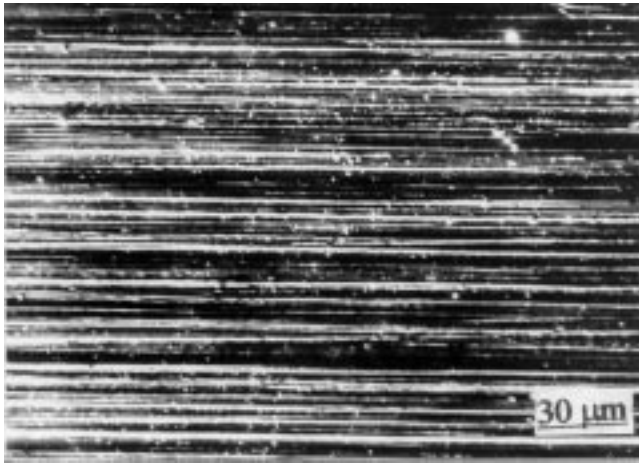


**Fig. 11** Micrograph of the wear surface of hardfacing material of composition 2

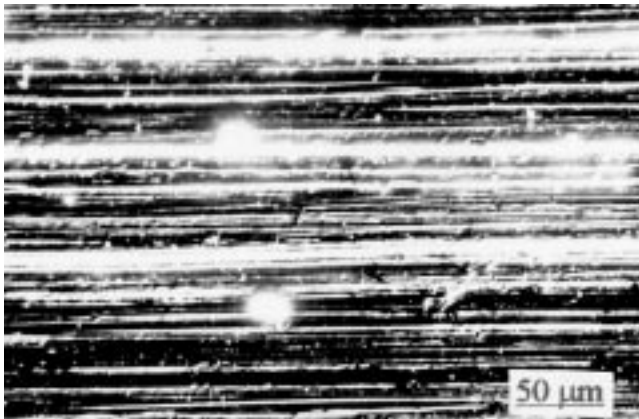


**Fig. 12** Micrograph of the wear surface of hardfacing material of composition 3

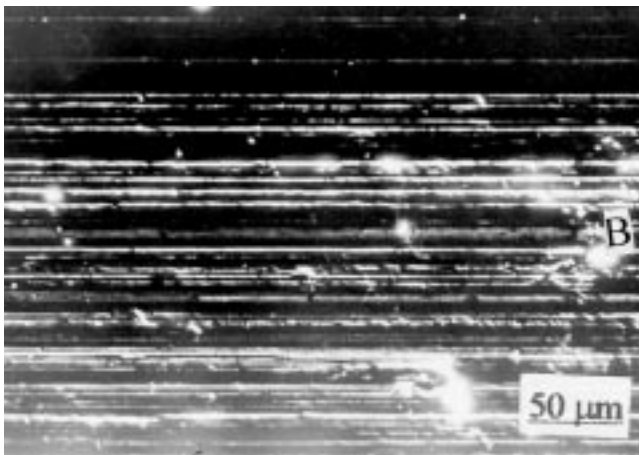


**Fig. 13** The wear surface of overlaid alloy composition 3 showing shallower continuous wear groove

material. During ploughing, generally, material from the wear grooves is displaced along the wear tracks in the form of flakes. The relative amount of cutting and ploughing depends on the material characterization and experimental parameters such as load and abrasive size. In this investigation, the abrasive size and load are constant. The ploughing action becomes predominant when the material is softer, as in the case of mild steel. Thus, the formation of deeper grooves was taking place. The cutting action becomes dominant when the material is harder, as in the case of overlaying material of composition 1. However, both these mechanisms, cutting and ploughing, were taking place simultaneously in each material. The mild steel contains a ferrite-pearlitic structure, which has higher ductility and lower hardness, causing ploughing to become the dominating wear mechanism, whereas overlaying material of composition 1 causes cutting to be the dominating wear mechanism.

#### 4. Conclusions

The wear rates of the hardfacing/overlaying alloys are lower than that of mild steel. The minimum wear rate was observed in the case of overlaying material of composition 1. This may be due to the finer microstructure and the presence of more primary and secondary carbides (6.5%). Among the hardfacing materials of compositions 2 and 3, the former gives marginally greater wear resistance than the latter. This may be due to the occurrence of a Widmannstapan type of structure in a few areas of composition 3 and relatively coarser bainite. The abrasive wear mechanism is associated with both cutting and ploughing action by the abrasive particles. Basically, the nature of the groove and material removal mechanism depends upon the hardness and microstructural characteristics of the material. When hardness is lower, as in case of mild steel, the ploughing mechanism is dominating. At the intermediate hardness (compositions 2 and 3), both cutting and ploughing simultaneously take place. But at the higher hardness, the cutting mechanism dominates. The wear mechanism is also associated with clogging, capping, and fracturing of abrasives and work hardening of the surface of the workpiece.

#### References

1. D. Bohme and F. Prultmann: *Proc. Surface Eng. Conf., Bombay*, 1985, vol. 1, p. 33.
2. B. Bhusan and B.K. Gupta: *Handbook of Tribology—Material Coating and Surface Treatments*, McGraw-Hill, New York, NY, 1991, p. 81.
3. M.A. Clegg, R.C. Cooki, and R.W. Frases: *Metals Handbook*, ASM, Materials Park, OH, 1992, vol. 9, p. 18.
4. F. Hobart: *Welding Rev. Int.*, 1983, vol. 22, pp. 18-22.
5. G. Sundararajan: *J. Metall. Mater. Proc.* 1994, vol. 5, pp. 215-32.
6. Weite Wu and Lung-Tien Wu: *Metall. Trans A*, 1986, vol. 27A, pp. 3639-46.
7. J.E. Hinkel: *Maintenance Welding, Handbook of Maintenance Engineering*, McGraw-Hill Book Company, New York, NY, 1973, pp. 15-1-15-50.
8. *Metals Handbook*, 9th ed., ASM Materials Park, OH, 1972, vol. 7, pp. 563-67.
9. *Metals Handbook*, 9th ed., ASM Materials Park, OH, 1972, vol. 7, pp. 770-86.
10. B.K. Prasad, S.V. Prasad, and A.A. Das: *J. Mater. Sci.*, 1992, vol. 27, p. 4489.

11. G. Sundararajan: *J. Met. Mater. Proc.* 1993, vol. 4, pp. 162-64.
12. B.K Prasad, K. Venkateshwarlu, O.P. Modi, and A.H. Yegneswaran: *J. Mater. Sci. Lett.*, 1996, vol. 15, pp. 1773-76.
13. M.M. Khrush Chov: *Wear*, 1974, vol. 28, pp. 59-72.
14. B.K. Prasad and S.V. Prasad: *Wear*, 1991, vol. 151, pp. 1-9.
15. L. Fang and Q.D. Zhaou: *Wear*, 1991, vol. 151, pp. 313-23.
16. B.K. Prasad, S. Das, A.K. Jha, O.P. Modi, R. Dasgupta, and A.H. Yegneswaran: *Composite, Part A*, 1997, vol. 28A, pp. 301-38.
17. R. Dasgupta, B.K Prasad, A.K Jha, O.P. Modi, S. Das, and A.H. Yegneswaran, *Wear*, 1997, vol. 209, pp. 255-62.